https://bjas.journals.ekb.eg/

engineering sciences

# The Influence of FDM Process Parameters on The Tensile Strength in an Open-Hole Test

Ahmed Elkhwaga, Abdalla M. Abdalla and Saleh Kaytbay

Department of Mechanical Engineering, Faculty of Engineering, Benha University.

Email: ahmed.alkhawaga@bhit.bu.edu.eg

#### Abstract

The advantages of additive manufacturing technology have a big influence on various industrial applications. The use of 3D printing technology facilitates the creation of complex, lightweight geometric designs with increased robustness. This study focuses on the effect of recommended parameters of printing like raster angle  $(45^{\circ}/-45^{\circ}, 0^{\circ}/90^{\circ})$ , layer thickness (0.2, 0.15, and 0.1 mm), and infill pattern (cross 3D and gyroid) on the tensile strength and other mechanical properties of the open-hole test. The specimens were fabricated utilizing Fused Filament Fabrication (FFF) technology using Poly-Lactic Acid (PLA) thermoplastic material by a 3D printer machine in a standard dimension. According to the test results, the tensile strength and other mechanical properties were strongly impacted by the parameters. The best results were obtained with a 45/-45 raster angle, 0.1 mm layer thickness, and a gyroid infill pattern, and the tensile strength as a result was 27.6 MPa, strain was 8.24%, and elongation was 12.35 mm.

Keywords: FDM, Raster Angle, Layer Thickness, Infill Pattern, Tensile Strength, Open-Hole Test.

#### 1. Introduction

3D printing is an additive manufacturing process in which a tangible object is produced from a digital three-dimensional model. This innovative technique involves the sequential layering of materials, such as plastics, metals, or composites, to construct a physical representation of the virtual design. Fused Deposition Modeling (FDM) is the most widely utilized 3D printing technique, involving the construction of a part by extruding a polymer filament in a molten state. [1]. The primary advantages of fused deposition modeling technology support an extensive variety of plastic and composite materials, facilitate straightforward material swaps, incurs minimal maintenance expenses, enables swift production of parts, utilizes environmentally safe and non-toxic materials, features a compact design, and operates efficiently at low temperatures. Fused deposition modeling utilizes an extrusion nozzle to heat the material, causing it to transition into a molten state, enabling the sequential layering of material. Each new layer is deposited onto the previous one, ensuring the progression of the manufacturing process while maintaining the designated geometry. Plastic filaments composed of (PLA) and Acrylonitrile butadiene styrene (ABS) are commonly employed in the fused deposition modeling technique. Many factors significantly influence the built parts' characteristics and manufacturing efficiency. Key variables impacting the 3D printing process include layer height, part orientation, raster angle, infill density, printing speed, extrusion temperature, raster width, air gap, and contour number.

The layer thickness refers to the measurement of the deposited layer's height in the vertical direction (Z-direction) after extrusion from the tip of the nozzle in an FDM machine. [2]. De Toro et al. [3] demonstrated in their experimental experiments that layer height has a significant impact on the bending strength and impact resistance of the fabricated part.

For Part Orientation, the part's orientation within the FDM printer refers to its positioning relative to the X, Y, and Z axes, including the orientation angle at which the part is fabricated. Kumar et al. [4] demonstrated that the maximum tensile strength is attained when the build orientation angle is set to zero. Moreover, it is greater for a raster angle of zero and for a smaller layer thickness.

print: ISSN 2356-9751

online: ISSN 2356-976x

For extrusion temperature, this characteristic depends on the specific thermoplastic material used for printing. It influences the material's viscosity during the printing process, thereby influencing the properties of the final component. The presence of internal stress can cause deformation inside the layers of the material, which in turn might lead to the failure of the produced part. Increasing the extrusion temperature results in an increase in the tensile strength [4].

The speed at which the extruder travels along the XY-plane during extrusion is called printing speed. The rate at which printing occurs significantly influences the distortion of the construction component [5].

The infill density denotes the proportion of filament material within the infill volume of part. The strength of an object is influenced by its infill density. End-use items are typically preferred to have a higher infill density [6]. The improved tensile strength can be attributed to increased infill density and decreased layer thickness [7].

Raster Angle is the angle at which the deposited material is deposited on the build platform, relative to the X-direction.

The width of the beads is determined by the deposition along the extrusion tool path, which ultimately forms the raster is called raster width. A wider raster width achieves the greatest tensile strength [4].

The term refers to the period between two consecutive bead depositions, the air gap.

Contour number refers to the quantity of solid layers that enclose the interior infill pattern or structure of the item produced by FDM.

#### 2. Open-hole tensile test

Considering that some 3D-printed plates with open holes may experience tensile loads during their operational use, it is important to investigate the mechanical strength of these components. The specimens in this study were fabricated using the Fused Deposition Modeling (FDM) method with (PLA) as the material. Alongside experimental testing, numerical simulations were conducted to validate the findings, leading to a strong correlation between the experimental results and the simulation outcomes.

The specimen for the open-hole tensile testing is fabricated according to the ASTM D5766 standard. According to this standard, the sample is a rectangular plate featuring a centrally located hole, as illustrated in Figure 1.

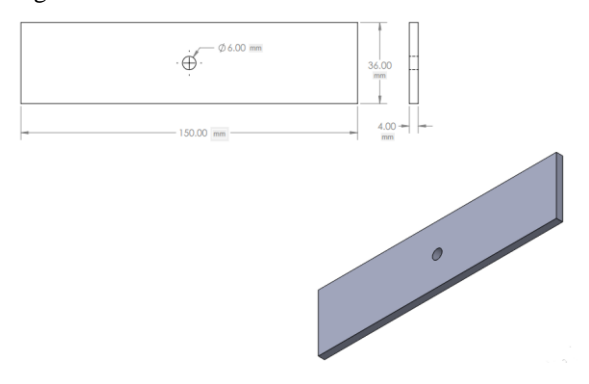
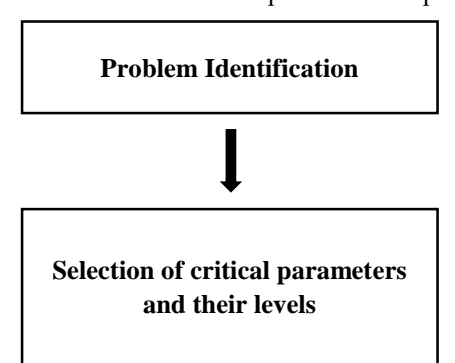


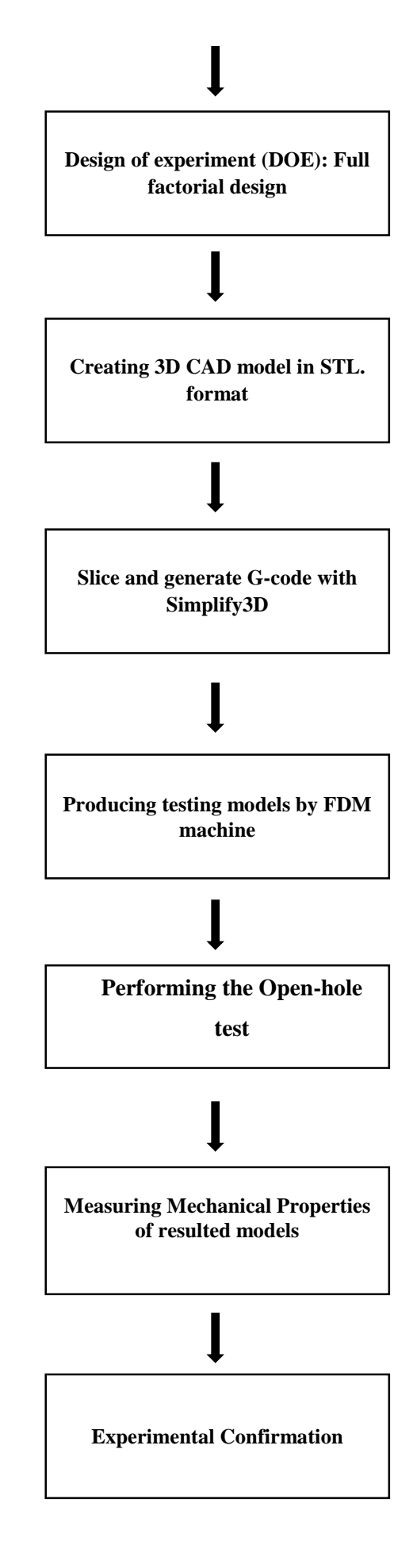
Fig (1) FDM model sample.

## 3. Material and Methods

The relationship between the mechanical characteristics of the output part, tensile strength, and the flexible parameters for raster angle, layer thickness, and infill pattern is the primary target of the current study. Consequently, the testing phases were outlined in a systematic fashion. Selecting the FDM variable process parameters and their corresponding levels was the initial step. subsequently generating a statistical design of experiment (DOE).

The flowchart of the experimentation plan.





The experiment is conducted using a 3D printing machine that utilizes a (PLA) polymer with a diameter of 1.75 mm as the building material. PLA's superior tensile strength, minimal warping, and low ductility compared to ABS make it the preferred choice [8]. Additionally, PLA is simpler to print on and offers a superior surface polish. [9].

The sample is prepared as a three-dimensional (3D) model using commercial computer-assisted design (CAD) software (SolidWorks, 2021). The model is

saved in stereolithography (STL) format, which can be read by the FDM machine. Subsequently, export the STL file to the operational program, Simplify3D. During this phase, the part undergoes slicing to a specific thickness, generating the G-code.

The model is fabricated using the FDM machine, following the necessary adjustments to the machine configuration. Now preparing the model sample extracted from the machine for measurement.

Table (1) PLA filament characteristics

Properties	Range	Unit	
Printing Temperature	190 - 210	Celsius	
Bed temperature	60 – 80 Celsiu		
Density	1.25	g/cm <sup>3</sup>	
Tensile Strength	65	MPa	
Elongation at Break	8	%	
Flexural Strength	97	MPa	
Flexural Modulus	3600	MPa	
IZOD Impact Strength	4000	$J/m^2$	

**Table (2)** Levels of fixed parameters

Parameter	Level	Unit
Infill Density	60	%
Printing Temperature	205	Celsius
Bed Temperature	65	Celsius
Printing speed	60	mm/s
Top and bottom Layers	4	number

Table (3) Levels of process parameters

Symbol	Parameter	Unit	Level 1	Level 2	Level 3
a	Raster angle	degree	45°/-45°	0°/90°	-
b	Layer Height	mm	0.1	0.15	0.2
c	Infill pattern	-	Cross 3D	Gyroid	-

Table (	<b>(4</b> )	Experimental	Design
Lant	T,	LADCITICITAL	DUSIEII

	Control Parameters					
Sample No.	Raster angle	Layer Height	Infill pattern			
1	45°/-45°	0.2	Cross 3D			
2	45°/-45°	0.15	Cross 3D			
3	45°/-45°	0.1	Cross 3D			
4	45°/-45°	0.2	Gyroid			
5	45°/-45°	0.15	Gyroid			
6	45°/-45°	0.1	Gyroid			
7	0°/90°	0.2	Cross 3D			
8	0°/90°	0.15	Cross 3D			
9	0°/90°	0.1	Cross 3D			
10	0°/90°	0.2	Gyroid			
11	0°/90°	0.15	Gyroid			
12	0°/90°	0.1	Gyroid			

To assess tensile strength, twelve specimens were printed. Each test was replicated three times, resulting in a total of 36 tests.

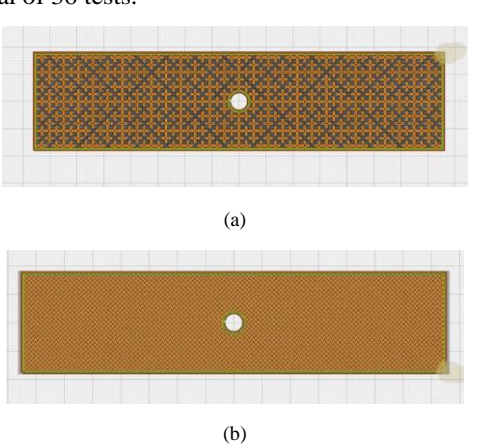
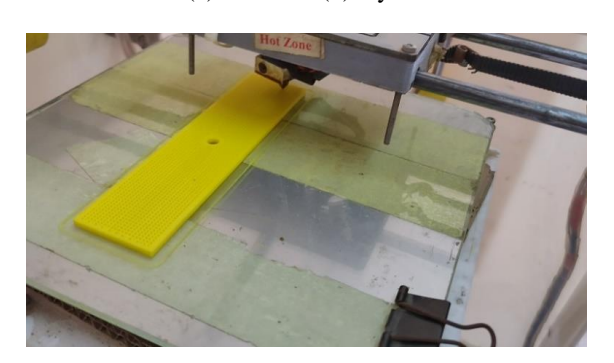


**Fig (2)** The infill pattern's geometrical arrangement (a) Cross3D (b) Gyroid.



Fig~(3) using a 3D printer to create the specimen.

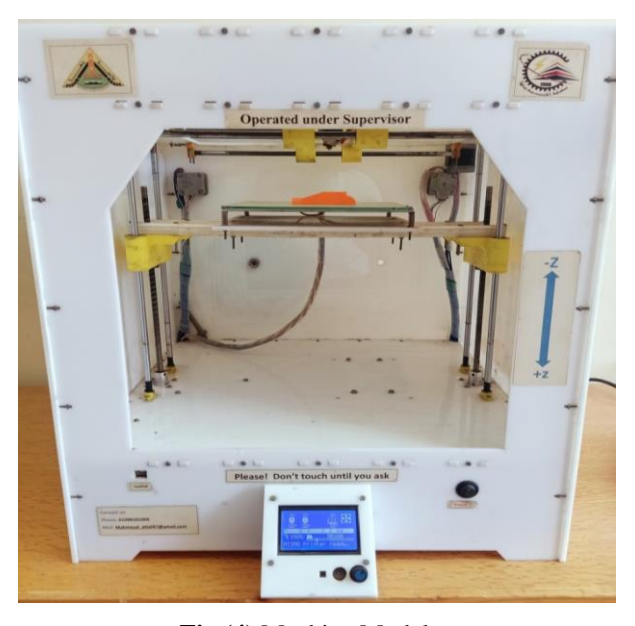


Fig (4) Machine Model.

Table (5) Machine specifications

Specification	Description		
Technology for Printing	Fused deposition modelling (FDM)		
Connectivity	SD card or USB flash drive		
Nozzle Temperature	Up to 245 °C		
Layer Resolution	20 – 200 microns		
Build Volume	180 x 180 x 290 mm		
Print Speed	30 - 200 mm/s		
Nozzle Diameter	0.4 mm		
Power Source	Electric (220–240 V)		

## 4. Results and Discussions

Table 6 shows the average results of the experimental tensile strength test under various control parameters, including Raster angle ( $45^{\circ}$ /- $45^{\circ}$ ,  $0^{\circ}$ /90°), Layer thickness (0.2,0.15, and 0.1mm), and Infill pattern (cross 3D and gyroid).

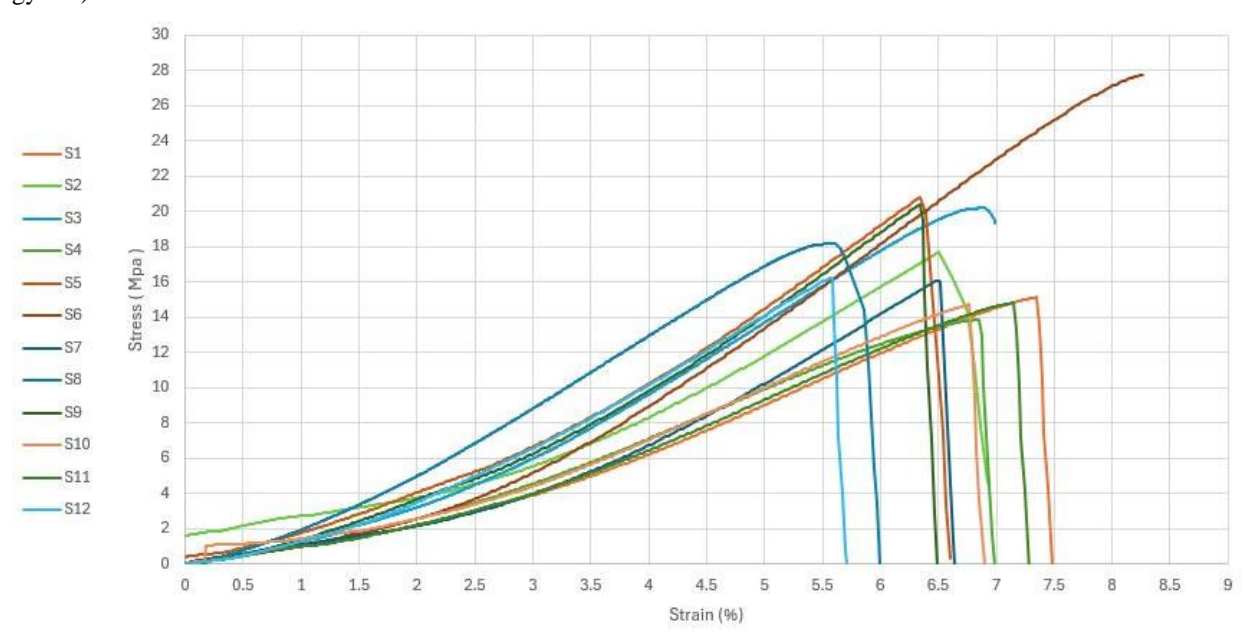


Fig (5) Average Stress-Strain curve for samples.



Fig (6) Fabricated Tension Test samples.

Table (6) Results

	Control Parameters							
Sample No.	Raster angle	Layer Height	Infill pattern	Time (hour)	Weight (gram)	UTS (MPa)	Fracture Strain (%)	Elongation (mm)
1	45°/-45°	0.2	Cross 3D	1:12	20.88	15.1	7.35	11.02
2	45°/-45°	0.15	Cross 3D	1:29	20.3	17.7	6.51	9.75
3	45°/-45°	0.1	Cross 3D	2:01	19.15	20.2	6.88	10.32
4	45°/-45°	0.2	Gyroid	1:25	19.68	13.8	6.85	10.27
5	45°/-45°	0.15	Gyroid	1:47	18.88	21.8	6.34	9.51
6	45°/-45°	0.1	Gyroid	2:34	17.55	27.7	8.24	12.35
7	0°/90°	0.2	Cross 3D	1:11	20.65	16.1	6.51	9.75
8	0°/90°	0.15	Cross 3D	1:28	20.06	18.2	5.57	8.36
9	0°/90°	0.1	Cross 3D	1:57	18.89	20.4	6.34	9.51
10	0°/90°	0.2	Gyroid	1:24	19.67	14.7	6.77	10.15
11	0°/90°	0.15	Gyroid	1:48	18.89	14.8	7.15	10.72
12	0°/90°	0.1	Gyroid	2:33	17.57	16.2	5.58	8.37

The trial version of Design-Expert® was used to conduct a statistical analysis of the data as follows:

#### 4.1. Analysis results for tensile strength

## 4.1.1. Analysis of variance (ANOVA)

Analysis of variance (ANOVA) was used to examine test result data to determine the effects of an internal factor of raster angle, layer thickness, and infill pattern on specimen tensile test value. This analysis is a computational method that, by identifying hypotheses on the impact of variables under control and how they interact as shown in Table 7.

### 4.1.2. The final formula using the code factors

Tensile strength = 
$$18.08 - 1.32^{\circ}A - 3.14*B + 0.0667*B^2 + 0.1111*C + 1.78*AB - 0.3167*AB^2 - 1.59*AC - 0.7861*BC + 0.0889*B^2C$$
 (1)

By comparing the factor coefficients, the formula in terms of the coded factors can be used to forecast the response for specific levels of each element and to determine the relative importance of the factors.

## 4.1.3. Model Validation

One method to evaluate the experiment's design's validity is the examination of residuals. Figure 7 shows the plots of residuals for tensile strength. It is evident from these statistics that the residuals exhibit standard behaviour.

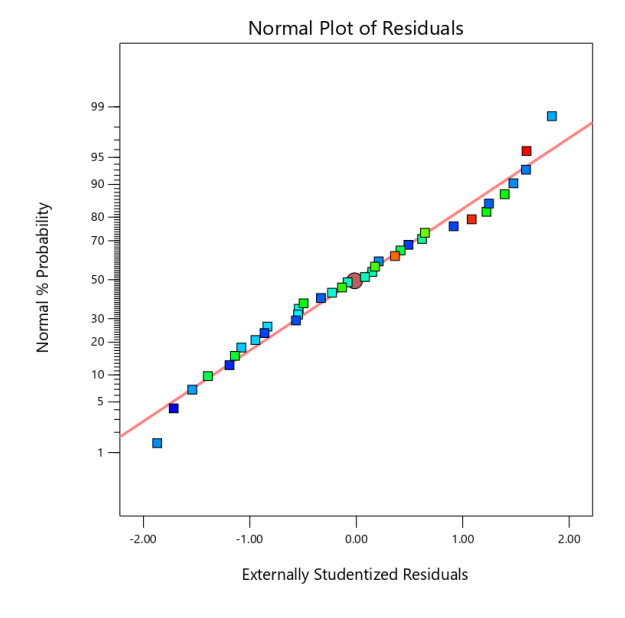


Fig (7) Residuals for Tensile Strength.

The straight line's data points show the residuals' independence and normalcy, and their usual behaviour is apparent.

Comparing experimental data with the model's predictions is an additional method of evaluating the regression model's fit to the data. Because the dots in figure 8 are so close to the diagonal. There is a strong connection between data from experiments and the tensile strength data generated by the statistical model.

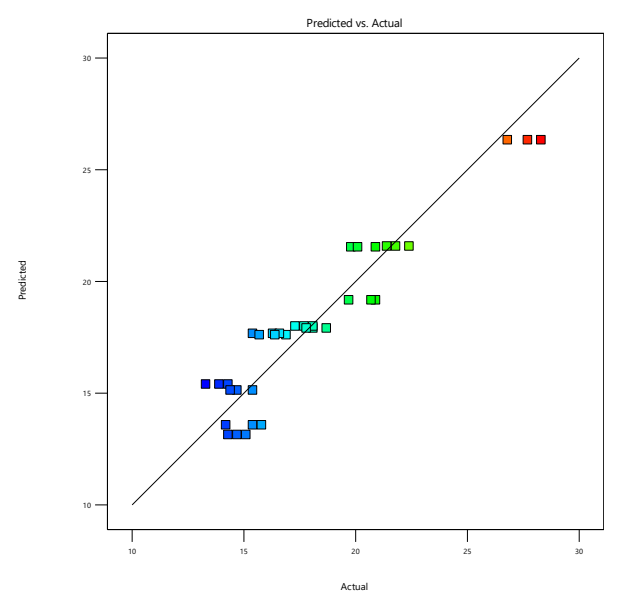


Fig (8) Predicted and Experimental Data for Tensile Strength.

Source	Sum of Squares	df	Mean Square	F-value	p-value	
Model	463.58	9	51.51	23.16	< 0.0001	significant
A-Raster Angle	62.41	1	62.41	28.06	< 0.0001	
B-Layer Thickness	231.96	2	115.98	52.14	< 0.0001	
C-Infill Pattern	0.4444	1	0.4444	0.1998	0.6586	
AB	64.53	2	32.27	14.51	< 0.0001	
AC	90.88	1	90.88	40.86	< 0.0001	
BC	13.34	2	6.67	3.00	0.0673	
Residual	57.83	26	2.22			
Lack of Fit	49.73	2	24.86	73.61	< 0.0001	significant
Pure Error	8.11	24	0.3378			
Cor Total	521.41	35				

Table (7) Tensile Strength ANOVA Results

## 5. Conclusion

The impact of raster angle, layer thickness, and infill pattern on the tensile strength of open-hole specimens is examined in the current study using a full factorial experiment.

Parameters (raster angle, layer thickness, and infill pattern) have substantial impact on the tensile strength of open hole test as layer thickness has the greatest effect on tensile strength. The main effect is as follows:

- **a.** The open hole specimen's maximum tensile strength was noted at  $45^{\circ}/-45^{\circ}$  raster angle, 0.1 mm layer thickness, and gyroid infill pattern.
- **b.** The most influenced parameter on tensile strength is layer thickness.
- **c.** It is discovered that the samples with gyroid infill pattern have a greater ultimate tensile strength than those with cross 3D infill patterns in most samples.
- **d.**The layer thickness with 0.1 and 0.15mm provides higher tensile strength than the 0.2 mm for the same pattern.
- **e.** It was also observed that the raster angle 45°/-45° showed higher UTS than the 0°/90° one in most samples.
- **f.** The most influenced parameter on weight is layer thickness.

- **g.** The open hole specimen's minimum weight was noted at  $45^{\circ}/-45^{\circ}$  raster angle, 0.1 mm layer thickness, and gyroid infill pattern.
- **h.** The most influenced parameter on time is layer thickness.
- i. There was substantially less time for the open hole specimen at  $0^{\circ}/90^{\circ}$  raster angle, 0.2 mm layer thickness, and Cross 3D infill pattern.

#### References

- [1] C.K. Chua, K.F. Leong, C.S. Lim, 2003, Rapid Prototyping: Principles and Applications, second edition, World Scientific Publishing Co Inc, Singapore.
- [2] Deshwal, S., Kumar, A., and Chhabra, D., 2020 "Exercising hybrid statistical tools GA-RSM, GA-ANN and GA-ANFIS to optimize FDM process parameters for tensile strength improvement," CIRP Journal of Manufacturing Science and Technology, vol. 31, pp. 189-199.
- [3] De Toro, E. V., Sobrino, J. C., Martínez, A. M., and Eguía, V. M., 2019 "Analysis of the influence of the variables of the Fused Deposition Modeling (FDM) process on the mechanical properties of a carbon fiber-reinforced polyamide," Procedia Manufacturing, vol 41, pp. 731-738.
- [4] Sheoran, A. J., and Kumar, H., 2020 "Fused Deposition modeling process parameters

- optimization and effect on mechanical properties and part quality: Review and reflection on present research," Mater. Today Proceed, vol. 21, pp. 1659-1672.
- [5] Kačergis, L., Mitkus, R., and Sinapius, M., 2019 "Influence of fused deposition modeling process parameters on the transformation of 4D printed morphing structures," Smart Materials and Structures, vol. 28, no. 10.
- [6] Alsoufi, M. S., and Elsayed, A. E.,2018 "Surface roughness quality and dimensional accuracy-a comprehensive analysis of 100% infill printed parts fabricated by a personal/desktop cost-effective FDM 3D printer," Materials Sciences and Applications, vol. 11, no. 1.
- [7] Srinivasan, R., Pridhar, T., Ramprasath, L. S., Charan, N. S., and Ruban, W., 2020 "Prediction of tensile strength in FDM printed ABS parts using response surface methodology (RSM)," Materials today, vol. 27, pp.1827-1832.
- [8] Kim, H., Park, E., Kim, S., Park, B., Kim, N., and Lee, S., 2017 "Experimental study on mechanical properties of single-and dualmaterial 3D printed products," Procedia Manufacturing, vol. 10, pp. 887-897.
- [9] Sheoran, A. J., and Kumar, H., 2020 "Fused Deposition modeling process parameters optimization and effect on mechanical properties and part quality: Review and reflection on present research," Mater. Today Proceed, vol. 21, pp. 1659-1672.